Role of Unusual Amino Acid Residues in the Proximal and Distal Heme Regions of a Plant P450, CYP73A1[†]

Michel Schalk,[‡] Svetlana Nedelkina,[§] Guillaume Schoch,[‡] Yannick Batard,[‡] and Danièle Werck-Reichhart*[,‡]

Département d'Enzymologie Cellulaire et Moléculaire, Institut de Biologie Moléculaire des Plantes, Centre National de la Recherche Scientifique UPR 406, 28 rue Goethe, 67000 Strasbourg, France, and Institute of Cytology and Genetics, 630090 Novosibirsk-90, Russia

Received December 18, 1998; Revised Manuscript Received March 17, 1999

ABSTRACT: CYP73A1 is a typical plant P450 in terms of its function and primary sequence. The enzyme catalyzes the 4-hydroxylation of *trans*-cinnamic acid, the first oxidative step in the phenylpropanoid pathway. Its primary protein sequence exhibits some particular landmarks which are characteristic of plant P450 enzymes. The most interesting is a proline residue (Pro448), very unusual in animal P450s, just C-terminal to the invariant heme-binding cysteine. To determine the role of this proline, we substituted it with valine, isoleucine, or phenylalanine, residues found in animal P450s, using site-directed mutagenesis. Expression of the wild type and mutants in yeast indicated that replacement of Pro448 led to disruption of the heme−protein interaction, loss of catalytic activity, and either impaired expression or destabilization of the apoprotein. Pro448 is thus essential for the correct insertion of heme in the apoprotein. Another typical feature of CYP73A proteins is the presence of an alanine-alanine motif (Ala306-Ala307) on the presumed N-terminal edge of the cleft in the central part of the I helix. This cleft faces the iron on the distal side of the heme and is proposed to be essential for catalysis. Substitution of each or both Ala306 and Ala307 residues with glycines showed that they are critical for the stability of the protein and influence the positioning of the substrate in the active site. Results are discussed with reference to the structural X-ray data that are available for bacterial P450 proteins.

Cytochromes P450 form a large superfamily of more than 750 heme thiolate proteins (*1*). They catalyze monoxygenation of a remarkably broad range of chemicals, and are involved in metabolic pathways as well as in detoxification (or activation) of xenobiotics in all organisms. Most of them share common properties, i.e., heme and oxygen binding, electron transfer, and oxygen activation. Differences lie in the nature of the substrates which are oxidized. CYP73A1 is the first member of a family of orthologous enzymes that catalyze the 4-hydroxylation of *trans*-cinnamic acid to *p*-coumaric acid (*2*−*4*). Cinnamate 4-hydroxylase (C4H)[1] thus controls the first oxidative step in a plant specific pathway leading to the synthesis of lignin, flavonoids, coumarins, and other phenylpropanoids (*5*). The importance of this enzyme lies in the fact that it is involved in the biosynthesis of molecules that are essential for plant structure, development, and defense. From a phylogenetic point of view, CYP73A1 is a typical plant P450 and belongs to the large A group of plant enzymes which all derive from a common ancestor (*6*). This major group of plant P450s branches with CYP17, CYP21, and the large families of CYP1s and CYP2s.

Structural data that are available for P450 proteins all rely on X-ray crystal analysis of five soluble bacterial or fungal enzymes: $P450_{cam}$ (CYP101) from *Pseudomonas putida* (*7*), $P450_{BM-3}$ (CYP102) from *Bacillus megaterium* (*8*), $P450_{terp}$ (CYP108) from *Pseudomonas* sp. (*9*), P450eryF (CYP107A1) from *Saccharopolyspora erythraea* (*10*), and $P450_{NOR}$ from *Fusarium oxysporum* (*11*). Much of the understanding of the P450 mechanism is derived from studies with $P450_{cam}$ whose structure and biochemistry have been extensively studied (*12*). All crystallized P450s exhibit well-conserved secondary and three-dimensional structures (*10*, *13*). This is particularly true for the regions involved in heme binding (loop preceding proximal helix L) and oxygen activation (distal helix I).

Most eukaryotic P450s are bound to the endoplasmic reticulum or to the inner mitochondrial membrane. This results in some difficulties in obtaining the well-ordered crystals that are necessary for the analysis of their three-dimensional structure. Alternative experimental and analytical approaches to indirectly addressing the question, however, have provided a great deal of information. It is now well accepted that all P450s have a similar architecture (*13*−*16*). Both sequence and structural comparisons reveal highly conserved features, in particular in the C-terminal half of the proteins. A high degree of conservation is related to functions common to all P450s. The binding of heme to the thiolate side chain of a perfectly conserved cysteine provides

[†] M.S. was supported by the Ministère de la Recherche et de l'Enseignement Supérieur and S.N. by a Projet de Recherche Conjoint sur Convention Internationale of the Centre National de la Recherche Scientifique.

* Corresponding author. Telephone: (33) 3 88 35 83 32. Fax: (33) 3 88 35 84 84. E-mail: daniele.werck@ibmp-ulp.u-strasbg.fr.

[‡] Centre National de la Recherche Scientifique UPR 406.

[§] Institute of Cytology and Genetics.

[1] Abbreviations: C4H, *trans*-cinnamate 4-hydroxylase [NADPH: oxygen oxidoreductase (4-hydroxylating), EC 1.14.13.11]; HS, high-spin.

10.1021/bi982989w CCC: $18.00
Published on Web 04/24/1999

Table 1: Primary Amino Acid Sequence of the Conserved Heme-Binding Region in CYP73A1 and Some Other P450 Proteins[a]

P. putida CYP101 (cam)	T	*F*	*G*	H	*G*	S	H	L	*C*	**L**	*G*	Q	H	L	A
B. megaterium CYP102 (BM-3)	P	*F*	*G*	N	*G*	Q	R	A	*C*	**I**	*G*	Q	Q	F	A
Pseudomonas sp. CYP108 (terp)	G	*F*	*G*	W	*G*	A	H	M	*C*	**L**	*G*	Q	H	L	A
Saccharopolyspora erythraea CYP107A1 (eryF)	S	*F*	*G*	Q	*G*	I	H	F	*C*	**M**	*G*	R	P	L	A
trout CYP2M1	A	*F*	*G*	V	*G*	K	R	A	*C*	**P**	*G*	E	A	L	A
new human P450	A	*F*	*G*	A	*G*	S	S	Q	*C*	**P**	*G*	K	V	F	A
rat CYP7A1	P	*F*	*G*	S	*G*	A	T	I	*C*	**P**	*G*	R	L	F	A
A. tumefaciens CYP104	S	*F*	*G*	C	*G*	P	H	H	*C*	**P**	*G*	A	Q	I	S
Z. mays CYP78A1	P	*F*	*G*	A	*G*	R	R	V	*C*	**P**	*G*	K	M	L	G
Berberis stolonifera CYP80	P	*F*	*G*	S	*G*	R	R	I	*C*	**P**	*G*	R	P	L	A
Persea americana CYP71A1	P	*F*	*G*	A	*G*	R	R	G	*C*	**P**	*G*	I	A	F	G
Z. mays CYP88	A	*F*	*G*	L	*G*	A	R	L	*C*	**P**	*G*	N	D	L	A
Arabidopsis thaliana CYP90	P	*F*	*G*	G	*G*	P	R	L	*C*	**P**	*G*	Y	E	L	A
Helianthus tuberosus CYP73A1	P	*F*	*G*	V	*G*	R	R	S	*C*	**P**	*G*	I	I	L	A
residue in the CYP73A1 sequence									*447*	**448**					
		−7							*C*	**+1**	*+2*				

[a] Bold letters denote the amino acids which have been modified in this study. The italic areas correspond to the residues highly conserved in P450 proteins. Sequences have been selected in data banks so as to show all non-plant and a representative sampling of plant P450s with a proline in C+1 relative to the heme-binding cysteine.

Table 2: Primary Amino Acid Sequence in the Conserved Functional Region of the I Helix of CYP73A1 and Some Other P450 Proteins[a]

P. putida CYP101 (cam)	G	L	L	L	V	**G**	**G**	L	*D*	*T*	V	V
B. megaterium CYP102 (BM-3)	I	T	F	L	I	**A**	**G**	H	*E*	*T*	T	S
Pseudomonas sp. CYP108 (terp)	V	A	I	A	T	**A**	**G**	H	*D*	*T*	T	S
Sa. erythraea CYP107A1 (eryF)	L	V	L	L	L	**A**	**G**	F	*E*	*A*	S	V
Rhodococcus sp. CYP116	F	G	G	V	F	**A**	**A**	H	*E*	*T*	T	T
rat CYP7A1	L	A	I	L	W	**A**	**S**	Q	*A*	*N*	T	I
human CYP24	T	E	L	Q	L	**A**	**A**	V	*E*	*T*	T	A
L. stagnalis CYP10	V	D	L	M	L	**A**	**A**	V	*E*	*T*	T	S
human CYP19	L	E	M	L	I	**A**	**A**	P	*D*	*T*	M	S
Sorghum bicolor CYP79	Q	D	I	T	F	**A**	**A**	V	*D*	*N*	P	S
Zea mays CYP71C1	V	N	M	F	E	**A**	**A**	I	*E*	*T*	S	F
Pe. americana CYP71A1	L	D	M	F	S	**G**	**G**	T	*D*	*T*	T	A
Petunia hybrida CYP75A1	L	N	L	F	T	**A**	**G**	T	*D*	*T*	S	S
Ar. thaliana CYP90	V	A	L	L	V	**A**	**G**	Y	*E*	*T*	T	S
H. tuberosus CYP73A1	E	N	I	N	V	**A**	**A**	I	*E*	*T*	T	L
residue in the CYP73A1 sequence						**306**	**307**			*310*		
						−4	**−3**	*−2*	*−1*	*T*		

[a] Bold letters denote the amino acids which have been modified in this study. The italic area corresponds to the threonine and T−1 acidic residue highly conserved in P450 proteins. Sequences have been selected so as to show all available P450s with an AA motif at positions T−3 and T−4.

spectral and catalytic properties to all P450 enzymes. This cysteine is flanked by a set of highly conserved residues usually considered the P450 signature F(G/S)xGx(H/R)-x**C**xGxx(I/L/F)A (Table 1) (*17*, *18*). Furthermore, the binding and activation of dioxygen (bond splitting) is a common catalytic step that is necessary for oxygen incorporation into all substrates. This property is associated with the presence of a distortion in the I helix which contributes to proton transfer and oxygen activation, and to another consensus sequence (A/G)(A/G)X(E/D)**T** characteristic of P450 enzymes (Table 2).

The role of different residues in these two regions has been extensively studied not only in the crystallized bacterial forms but also in membrane-bound P450s (*13*, *15*). A highly conserved threonine (bold character) plays a critical role in the I helix structure and function. It maintains a local deformation in the center of the helix by forming a hydrogen bond to a residue located four positions toward the amino terminus. This conserved threonine is also thought, maybe together with the adjacent acidic amino acid, to participate in oxygen activation by transferring protons from the surface of the protein to the iron-bound reduced dioxygen. Residues T−3 and T−4 are almost always glycine or alanine. In 71% of the available P450 sequences, these amino acids are A and G (T−4 and T−3), and in 12.6%, they are G and G. In all members of the CYP73A subfamily, both T−3 and T−4 residues are alanines. This pattern is very unusual and shared by only 5.5% of the registered P450s. In addition, crystallographic and mutagenesis data seem to suggest that the presence of a residue (a glycine or a proline) capable of inducing a bend in this region of the I helix is an important structural feature of P450 proteins (*19*). So why is such a residue not maintained in CYP73As?

On the heme proximal side, an invariant cysteine (bold in the consensus sequence) is the fifth ligand of the heme iron. The C+2 residue, except for one exception (the CYP79 family), is always a glycine. The amino acid flanked by these two conserved residues is more variable, but usually hydrophobic: L, I, V, A, or sometimes F or M. In CYP73As as well as in most plant P450s, a proline is found at C+1. When the local deformation and constraint usually induced by a proline in a protein structure is considered, the substitution for such an amino acid was unexpected. In addition, a cysteine with an adjacent proline was surprisingly reminiscent of the heme-binding motif found in many heme-regulated proteins (*20*).

Table 3: Sequences of the Oligonucleotides Used as Primers for Mutagenesis[a]

mutation	mutagenic primers	
	sense primers	reverse primers
Pro448Ile	5′-GAGTTGCATCGGGATTATTCTTGCATTG	5′-ATAATCCCGATGCAACTCCTTCTCCCGACTCC
Pro448Val	5′-GAGTTGCGTCGGGATTATTCTTGCATTG	5′-ATAATCCCGACGCAACTCCTTCTCCCGACTCC
Pro448Phe	5′-GAGTTGCTTCGGGATTATTCTTGCATTG	5′-ATAATCCCGAAGCAACTCCTTCTCCCGACTCC
Ala308Gly	5′-TTGCAGGAATCGAGACAACTC	5′-GAGTTGTCTCGATTCCTGCAACATTGATG
Ala307Gly	5′-ATGTTGGAGCAATCGAGACAAC	5′-TTGTCTCGATTCCTGCAACATTGATGTTTTC
Ala307Gly/Ala308Gly	5′-CAATGTTGGAGGAATCGAGACAACTCTA	5′-TAGAGTTGTCTCGATTCCTCCAACATTGATGTTTTCA

[a] Bases modified relative to the wild type sequence are underlined.

This paper describes our investigations on the role of the unusual residues found in the heme proximal and distal regions of the catalytic site of CYP73A1. Three mutants of the I helix and three mutants of the heme binding loop were generated by site-directed mutagenesis. The two alanines at positions T−4 and T−3 in the I helix were replaced by glycines, to obtain the Ala306Gly, Ala307Gly, and Ala306Gly/Ala307Gly mutants. Pro448 located just downstream of the invariant heme-binding cysteine was modified to generate the Pro448Ile, Pro448Val, and Pro448Phe mutants. Spectral and catalytic properties of the mutant and wild type CYP73A1s were compared after expression in yeast.

EXPERIMENTAL PROCEDURES

PCR. PCR mixtures (50 μL) contained each dNTP at 150 μM, each primer at 1 μM, 50 ng of template DNA, 1.25 units of Pfu DNA polymerase (Stratagene), 20 mM Tris-HCl (pH 8.75), 10 mM KCl, 10 mM $(NH_4)_2SO_4$, 2 mM $MgSO_4$, 0.1% Triton X-100, and 0.1 mg/mL bovine serum albumin. Reactions were performed in an M. J. Research PTC-150 Minicycler. The polymerase was added after preheating for 5 min at 92 °C. Thirty cycles of amplification (92 °C for 1 min, 52 °C for 2 min, and 72 °C for 2 min) were completed by 10 min of extension at 72 °C.

Site-Directed Mutagenesis. Mutant *CYP73A1* cDNAs were generated by PCR, using as a template the double-stranded wild type *CYP73A1* cDNA subcloned as an *Eco*RI−*Bam*HI fragment into the pBluescript SK phagemid. The procedure utilizes two universal primers flanking the *Eco*RI−*Bam*HI insert (T_3 and T_7), and two mutagenic primers overlapping the sequence to be modified, oriented in opposite directions, and complementary to each other for 18−28 nucleotides. The sequences of the primers used in our experiments are listed in Table 3. In a first step, two PCRs, one with T_3 and a mutagenic reverse primer and the other with T_7 and the corresponding mutagenic sense primer, were carried out simultaneously in two different tubes. This step provided two PCR products sharing a common sequence of 18−28 nucleotides and containing the desired mutation. These products were purified on 1% agarose gels before the second step; a single PCR was carried out using T_3 and T_7 as primers and 50 ng of each of the two previous PCR products as a template. This step provided a full-length cDNA with flanking *Eco*RI and *Bam*HI sites that was purified on agarose gel, digested, and ligated into shuttle vector pYEDP60. Clones of *Escherichia coli* transformed with this vector were first selected for correct size of their insert. Mutation of proline 448 in the heme-binding domain leads to the loss of a unique *Sma*I restriction site in the *CYP73A1* sequence. Mutants were thus selected for the absence of *Sma*I digests. Inserts exhibiting the expected modifications were fully sequenced, and only clones with no additional mutations were selected for expression in yeast.

C-Terminally 4His-tagged mutants were generated by PCR amplification of the modified sequences using the following primers: 5′GGGATCCCATGGACCTCCTCCTCATAGAA-AAAACCCTCGTCG3′ (sense) and 5′ATCGGAATTCCCT-TAATGATGATGATGAAATGACCTAGGTTTAGCTACG3′ (antisense). PCR products were fully sequenced. Despite the use of Pfu DNA polymerase, undesired mutation was obtained at this stage as stated in the Results.

Yeast Expression and Microsome Preparation. The modified *Saccharomyces cerevisae* W303-1B strain (*Mat a*; *ade2*-1; *his3*-11,-15; *leu2*-3,-112; *ura3*-1; *can*^{R}; *cyr*$^+$) overexpressing its own NADPH−P450 reductase under the control of the *GAL10-CYC1* promoter, also designated W(R), was constructed by Truan et al. (*21*). Plasmid C4H/V60, yeast transformation, and preparation of yeast microsomes were described by Urban et al. (*22*). Microsomes from the W(R) yeast strain transformed with the V60 void plasmid were used as a negative control.

For each construct, two independent transformed yeast clones were analyzed and all tests were carried out in duplicate.

Purification of the His-Tagged Protein. Yeast microsomes (20−200 mg of protein) resuspended in 0.1 M sodium phosphate (pH 7.5) containing 30% glycerol were solubilized by adding dropwise 1.25% (w/v) Emulgen 911 (Kao Atlas) and stirring on ice for 15 min. Samples were diluted with 1 volume of 0.05 M sodium phosphate (pH 7.5) containing 1 M NaCl and 10% glycerol, and centrifuged at 100000*g* for 45 min. The supernatant was applied at a flow rate of 0.1 mL/min to a 1 mL HiTrap chelating column (Pharmacia) complexed with Ni^{2+} according to the procedure recommended by the manufacturer and equilibrated in 0.05 M sodium phosphate (pH 7.5) containing 0.5 M NaCl and 10 mM imidazole (buffer A). The column was then washed with 30 mL of buffer A with 0.5% Emulgen 911 and 10% glycerol, and eluted with 10 mL of buffer A with 50 mM imidazole, 0.1% Emulgen 911, and 10% glycerol. The last 3 mL of the elution, containing a protein apparently devoid of contamination as determined on SDS gels, was pooled for heme determination. The purified protein was quantified using the Pierce BCA assay.

DNA and RNA Analysis. Isolation of yeast plasmid DNA was performed using the procedure described by Hoffman and Winston (*23*). Double-stranded plasmid DNA was sequenced using the prism Ready Reaction Dye Deoxy Terminator Cycle method of Applied Biosystems Inc., and

sequence data were analyzed using the GCG Sequence Analysis Software Package, version 8.1 (*24*).

The yeast RNA extraction protocol was adapted from Waldon and Lacroute (*25*). For Northern blotting, denatured RNA was separated in the presence of formaldehyde through a 1.2% agarose gel and transferred onto a nylon membrane Hybond N^+ (Amersham). RNA blots were prehybridized and hybridized with a *CYP73A1* full-length cDNA probe, radiolabeled with 50 μCi of [α-^{32}P]dCTP by random priming, at 65 °C according to established procedures (*26*). Membranes were washed twice for 10 min with 2× SSC and 0.1% SDS and once for 10 min with 0.2× SSC and 0.1% SDS at room temperature, and then twice for 30 min with 0.2× SSC and 0.1% SDS at 55 °C. The hybridization signal was recorded by autoradiography. RNA amounts were standardized by quantification of the ethidium bromide staining of the RNA gel before blotting.

Immunoblot Analysis. SDS−PAGE (10% total monomer, 0.3% cross-linker), electroblotting onto nitocellulose membranes (Hybond C, Amersham), and immunoblot staining using the rabbit polyclonal serum C4Hpa1 raised against purified *Helianthus tuberosus* C4H were performed as described by Werck-Reichhart et al. (*27*).

RNA Blot and Immunoblot Quantification. Blots and autoradiograms were scanned using an ARCUS II scanner and the Adobe Photoshop 3.0 program. Protein, transcripts, and total RNA were quantified using the NIH Image program, version 1.59.

Spectrophotometric Measurements and Catalytic Activity. Spectrophotometric measurements of total P450 (*28*) and P420 (*29*) content, evaluation of substrate binding (*30*), and measurements of NADPH oxidation (*22*) were performed as described previously. Heme content was estimated from the Soret absorption of the oxidized form of the purified protein, or by using the pyridine hemochrome assay as described in ref *31*.

trans-Cinnamic acid hydroxylation was assayed using radiolabeled *trans*-[3-^{14}C]cinnamic acid (Isotopchim, Ganagobie, France) as described previously (*32*). For the determination of kinetic constants, data were fitted using the nonlinear regression program DNRPEASY derived from DNRP53 (*33*).

Cytochrome P450 Sequences. P450 amino acid sequences and comparison in the proximal and distal heme regions were extracted from David Nelson's site on the World Wide Web server (http://drnelson.utmem.edu/nelsonhomepage.html).

RESULTS

Modification of Pro448 Located in the Heme-Binding Region. Proline 448, adjacent to the invariant heme-binding cysteine 447, was modified by PCR-directed mutagenesis to isoleucine, valine, or phenylalanine, three of the hydrophobic amino acids found in this location in non-plant and in some plant P450s. Following a control for undesired mutations, mutants and wild type cDNAs were cloned into shuttle plasmid pYeDP60 and expressed in a yeast strain engineered to overexpress its own reductase. The combination of this yeast strain and plasmid was previously shown to allow high levels of expression of CYP73A1 (*3*, *22*). Comparison of the expression, spectral properties, and catalytic activities of wild type and mutant proteins was

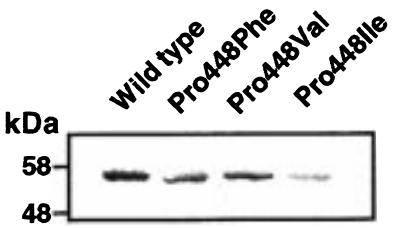

FIGURE 1: Immunoblot analysis of microsomal fractions from yeasts expressing wild type and Pro448 mutants of CYP73A1. Four micrograms of microsomal protein was loaded in each lane. The immunoblot was probed, with polyclonal antibodies were raised against C4H purified from tubers of *H. tuberosus*.

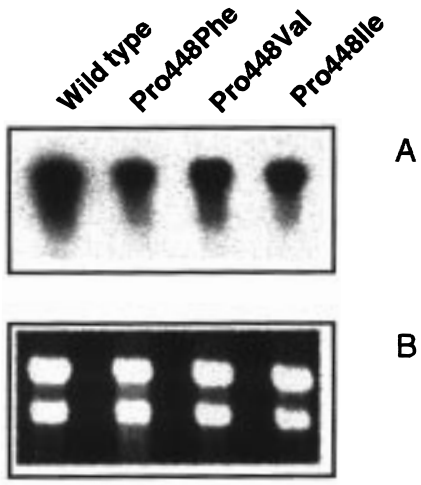

FIGURE 2: Steady state level of *CYP73A1* mRNA obtained after expression of the wild type and Pro448 mutants in *S. cerevisiae.* (A) Ten micrograms of total RNA was loaded in each lane. The blot was probed with a ^{32}P-radiolabeled full-length *CYP73A1* coding sequence. (B) Ethidium bromide staining of the RNA gel before blotting.

achieved using total RNA and microsomal membrane fractions of transformed yeasts prepared simultaneously under identical conditions of growth and induction.

The level of expression of the modified polypeptides was first determined by immunoblot analysis. SDS gel blots of transformed yeast microsomes were probed with polyclonal antibodies raised against purified *H. tuberosus* C4H (Figure 1). Quantification by densitometry of the immunodetectable protein indicated a ratio of the mutant to wild type enzyme of 0.39 for the Pro448Phe, 0.68 for the Pro448Val, and 0.09 for the Pro448Ile constructs. The Pro448 mutation thus resulted either in a decrease in the extent of CYP73A1 polypeptide synthesis or in accelerated protein degradation. The proline to valine mutation seemed to be less disruptive than the two other modifications. RNA blot analysis indicated a slightly lower steady state level of *CYP73A1* transcripts for the three mutants than for the wild type cDNA (Figure 2). Relative amounts of transcripts were 1, 0.55, 0.63, and 0.66 for the wild type and the Pro448Phe, Pro448Val, and Pro448Ile mutants, respectively.

The presence and correct orientation of heme in the active site was then investigated by differential spectrophotometry, monitoring spectral shifts of the Soret peak induced (i) by the binding of carbon monoxide to the reduced enzyme and (ii) by the binding of cinnamic acid to the native oxidized protein. Direct binding of CO as a sixth ligand to the iron is expected to occur if heme is present and reduced. It also

Table 4: Catalytic Activity of Wild Type and Pro448 Mutant Proteins[a]

	simple mutants				His-tagged mutants			
	wild type	Pro448Phe	Pro448Val	Pro448Ile	wild type	Pro448Phe	Pro448Val	Pro448Ile
P450 (pmol/mg)	795	10	137	7.8	762	60	15.4	3.7
P420 (pmol/mg)	0	27	0	18	0	75	36	42
P450 + P420	795	37	137	26	762	135	51.4	45.7
P450/P420	all P450	0.37	all P450	0.43	all P450	0.3	0.43	0.09
CYP73A1 (pmol/mg)	816	24	151	10.4	841	146	46.8	45.8
C4H activity (pkat/mg)	683 ± 23	24 ± 11	199 ± 3	6 ± 0.3	331 ± 14	80 ± 1	9 ± 3	5 ± 2
NADPH oxidation (pkat/mg)	763 ± 63	64 ± 25	378 ± 58	12 ± 3	377 ± 52	54 ± 22	nd[b]	nd
heme/protein ratio	−	−	−	−	0.41 ± 0.01	0.49 ± 0.02	0.30 ± 0.02	0.36 ± 0.02
relative level of protein expression (%)	100	39	68	9	100	57	47	34
relative no. of steady state transcripts	100	55	63	66	−	−	−	−

[a] The CYP73A1 content was determined from cinnamate-induced spectral changes, and P450 and P420 contents were determined from reduced/CO-bound minus reduced spectra. Spectral data are means of two measurements. Hydroxylation of *trans*-[^{14}C]cinnamic acid was measured using the assay described previously (*32*). Microsomes (50 μg/mL) were incubated in a final volume of 200 μL of sodium phosphate (pH 7.4) containing a saturating concentration (50 μM) of substrate, 500 μM NADPH, 5 mM glucose 6-phosphate, and 0.4 unit of glucose-6-phosphate dehydrogenase. CYP73A1-dependent NADPH oxidation was monitored by difference spectrophotometry at 350 nm, after addition of 50 μM cinnamate to the sample cuvette. The NADPH concentration was 500 μM, and the concentration of microsomal proteins was 50 μg/mL in this assay. The heme content was determined using the pyridine hemochrome assay. Values are means ± the standard deviation of three determinations. [b] nd, not detectable.

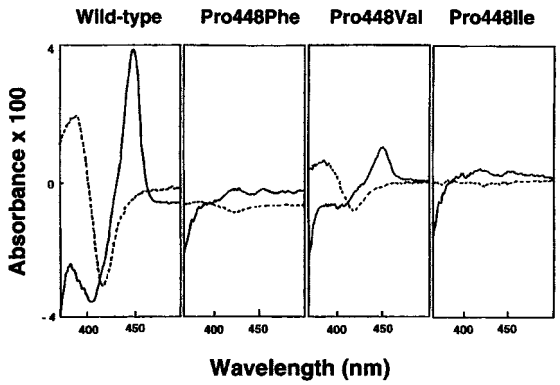

FIGURE 3: Reduced carbon monoxide difference spectra (—) and difference spectra induced by cinnamate binding (- - -) to oxidized microsomes derived from yeast cells expressing the wild type and Pro448 mutants of CYP73A1. Spectral analyses were conducted using identical amounts of microsomal proteins (0.6 mg/mL). Shifts induced by substrate binding were recorded in the presence of 100 μM cinnamic acid.

probably requires a correct orientation of the iron−porphyrin in the active site, since diatomic ligands such as CO or O_2 are expected to interact with amino acids located at the entrance of the I helix groove (*34*, *35*). The spectral shift resulting from the binding of substrate, on the other hand, reflects a change in the spin state (low- to high-spin) induced by the displacement of a molecule of water bound as the sixth ligand on the heme iron (*36*). Efficient displacement of water by cinnamate thus requires a perfect conservation of the spatial structure of the active site and of the distance between the substrate binding site and the heme iron. Figure 3 shows that CO and cinnamate bind the wild type enzyme, producing the expected shifts in the absorption maximum of the enzyme. Changes in heme absorbance resulting from the binding of both ligands to the Pro448Ile and Pro448Phe mutants decreased dramatically (Figure 3 and Table 4). A significant part of both mutants was detected as P420, an inactive form of P450 where the heme−thiolate bond is believed to be disrupted (*37*). Higher amounts of hemoprotein properly binding cinnamate and CO were found in microsomes of yeast expressing the mutant Pro448Val. This mutant P450 appeared to be more stable, and was not readily converted to P420.

These data were corroborated by measurement of catalytic activity. The activity was monitored following both NADPH oxidation induced by the addition of cinnamate and NADPH-dependent hydroxylation of radiolabeled *trans*-cinnamate in microsomes of transgenic yeast (Table 4). The rate of NADPH oxidation decreased to 8, 50, and 1.5% and *trans*-cinnamate hydroxylase activity to 3.5, 29, and 0.9% of the wild type rate when Pro448 was replaced by phenylalanine, valine, and isoleucine, respectively. Some of these activities were very low and near the detection limit of the assay.

Presence of Heme in the Pro448 Mutants. In mutants, activity and correct heme−ligand interactions decreased 2−10 times more than the immunodetected enzyme. The specific activities, expressed on the basis of the amounts of functional P450 present, were however similar to or greater than that of the wild type. This may be due to the absence of heme in a fraction of the apoprotein, but could also result from its incorrect orientation, preventing binding of substrate, O_2, and CO. To clarify this point, mutants tagged with four histidines at the C-terminus were generated, expressed in yeast, and purified by Ni^{2+}-affinity chromatography. According to the X-ray structure of the soluble P450s, the C-terminus of the protein is expected to be located at the surface of the cytoplasmic side of the folded polypeptide. The 4His tag should thus not interfere with the core structure of the active site and be accessible enough for purification without protein denaturation. It was, therefore, unexpected to observe a change in the relative expression of 4His-tagged mutants in yeast. Pro448Phe were slightly better expressed, the most significant changes being observed for Pro448Phe (Table 4). This effect may result from the aromatic character or positive charges of the four histidines at the surface of the protein. In the case of the Pro448Val mutant, an additional glycine to tryptophan mutation was found at Gly387 which may explain the decreased level of expression and stability of the protein.

The heme content of the purified proteins was determined from reduced versus oxidized pyridine hemochrome spectra (Table 4), similar results being obtained by direct measurement of the Soret absorbance of the ferric protein. Heme-to-protein ratios measured for mutants were about the same as that for the wild type. Small variations were observed

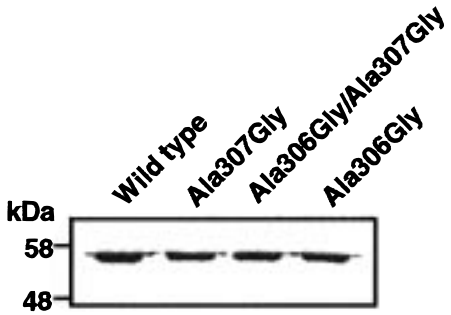

FIGURE 4: Immunoblot analysis of microsomal fractions from yeasts expressing the wild type and I helix mutants of CYP73A1. Four micrograms of microsomal protein was loaded in each lane. The immunoblot was probed with polyclonal antibodies raised against C4H purified from tubers of *H. tuberosus*.

among the mutants which roughly correlated to the relative level of expression and activity of the modified proteins. Despite a dramatic decrease in substrate and CO binding and catalytic activity, heme is thus present in all mutants.

Heme-to-protein ratios measured in this experiment, ranging from 0.3 to 0.49, were significantly smaller than the expected value of 1. This may result from some diffuse protein contamination, from a bias in the protein determination, or from the loss of heme induced by imidazole during the purification procedure. In this case, heme loss might depend on the change in amino acid.

Modifications of the I Helix. To determine the respective functional importance of the two alanines which are supposed to be forming the N-terminal border of the I helix cleft that are located three and four residues away from the conserved threonine in CYP73A1, we replaced them with glycines. Both the Ala307Gly and Ala306Gly single mutants, and the double Ala307Gly/Ala306Gly mutant, were generated. Comparison of the expression levels, spectral properties, and catalytic activities of the wild type and mutant proteins expressed in yeast was achieved like it was for mutants of the heme-binding region.

Immunoblot analysis, performed with microsomes of the transformed yeasts, indicated good expression of the modified proteins, although slightly lower quantities were produced than with the wild type (Figure 4). The ratios of mutant to wild type proteins quantified by densitometric scanning of the immunoblot were 0.70, 0.69, and 0.76 for the Ala307Gly, Ala306Gly, and double mutants, respectively. A reduced level of protein accumulation observed for the mutants did not result from a reduced level of message synthesis or stability since similar amounts of *CYP73A1* transcripts were detected in yeasts expressing the wild type and mutants (not shown). The presence of smaller amounts of CYP73A1 in microsomes from yeasts expressing the mutant proteins was confirmed by spectrophotometric analysis (Figure 5). The amounts of CO-binding P450 detected in the mutants relative to that in the wild type (0.75, 0.70, and 0.69 for the Ala307Gly, Ala306Gly, and double mutants, respectively) were in agreement with the immunoquantification of the protein.

To detect possible changes in the geometry of the active site and in the positioning of the substrate relative to heme iron, the $K_{s,app}$ and ΔA_{max} induced by cinnamate binding to the wild type were compared to those measured with the mutant proteins (Table 5). The affinity for cinnamate was

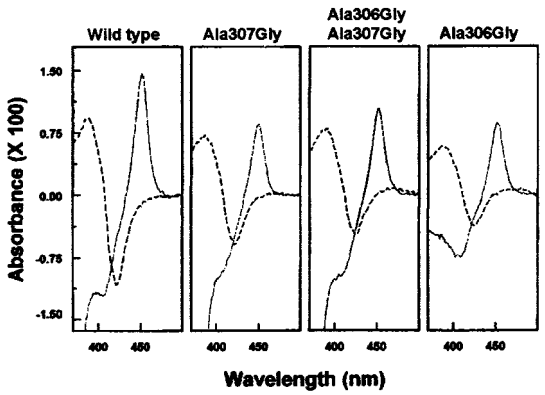

FIGURE 5: Reduced carbon monoxide difference spectra (—) and difference spectra induced by cinnamate binding to oxidized microsomes (- - -) derived from yeast cells expressing the wild type and I helix mutants of CYP73A1. Spectral analyses were conducted using identical amounts of microsomal proteins (0.4 mg/mL). Shifts induced by substrate binding were recorded in the presence of 100 μM cinnamic acid.

Table 5: Spectral Parameters of *trans*-Cinnamate Binding to the Wild Type and I Helix Mutants of CYP73A1[a]

	wild type	Ala307Gly	Ala307Gly/ Ala306Gly	Ala306Gly
$K_{s,app}$ (μM)	3.48 ± 0.25	1.85 ± 0.25	2.62 ± 0.42	4.92 ± 0.54
ΔA_{max}/P450 (A mmol^{-1})	123 ± 4	136 ± 9	100 ± 5	93.9 ± 8.5
% of HS	100	109 ± 7	81 ± 4	76 ± 7

[a] The apparent dissociation constant ($K_{s,app}$) for cinnamic acid and the maximum amplitude of the spectra at saturation were deduced from the variation in $\Delta A_{390-420}$ vs substrate concentration. Difference spectra were recorded with 0.4 mg/mL yeast microsomal protein in the cuvettes. P450 contents were calculated from the CO binding spectra. The percentage of high spin (% of HS) at the saturating concentration of substrate was calculated with reference to the wild type enzyme, assuming that a total low- to high-spin conversion was obtained in the case of wild type CYP73A1 (*22*).

increased in the case of the Ala307Gly and double mutants and decreased for the Ala306Gly protein, but these changes were not dramatic. The maximum amplitude of type I spectra resulting from the binding of substrate was also modified. If we assume that cinnamate is capable of totally displacing the solvent in the wild type CYP73A1 (*22*), the comparison of the ΔA_{max}/P450 ratios calculated for the mutants versus the wild type [expressed as a percentage of high-spin enzyme (% of HS)] should give an indication of the residual solvation of the active site after saturation by the substrate. As shown in Table 5, the % of HS measured for the Ala306Gly and double mutants indicated the presence of residual water in the active site. This is probably due to the nonoptimal orientation or increased mobility of the substrate. For the mutant Ala307Gly, in contrast, the % of HS reflected an ideal fit of the substrate in the active site.

The catalytic efficiency of the modified proteins was determined from measurements of the levels of *trans*-cinnamate hydroxylation and NADPH oxidation, the number of NADPH oxidized per substrate hydroxylated yielding information on the coupling of the reaction (Table 6). Differences in $K_{m,app}$ were small, but similar to those of $K_{s,app}$. They confirmed a small increase in the affinity for the Ala307Gly mutant. Differences in k_{cat} and coupling were more significant. The k_{cat} increased 37% for the Ala307Gly mutant and decreased about 75 and 50% for the Ala306Gly

Table 6: Comparison of the Catalytic Parameters of the Wild Type and I Helix Mutants of CYP73A1[a]

	wild type	Ala307Gly	Ala306Gly/Ala307Gly	Ala306Gly
$K_{m,app}$ (μM)	1.94 ± 0.26	1.66 ± 0.24	2.65 ± 0.30	2.82 ± 1.11
k_{cat} (min^{-1})	70.2 ± 1.7	96.2 ± 5.0	33.1 ± 1.9	16.0 ± 4.0
$k_{cat}/K_{m,app}$ (min^{-1} mM^{-1})	36	58	12	5.6
no. of NADPH oxidized per hydroxylated substrate	1.13 ± 0.06	1.24 ± 0.19	2.82 ± 0.20	5.31 ± 1.84

[a] Evaluation of activity was performed using transformed yeast microsomes. Assays for K_m and turnover determinations contained 500 μM NADPH, 5 mM glucose 6-phosphate, 0.4 unit of glucose-6-phosphate dehydrogenase, 25 μg/mL microsomal protein, 0.1 M sodium phosphate (pH 7.4), and 0.5−50 μM radiolabeled cinnamate in a final volume of 200 μL. The ratios of the extent of NADPH oxidation to cinnamate hydroxylation were calculated from assays using the same concentrations of NADPH (500 μM), substrate (50 μM), and enzyme (40 μg/mL of microsomal protein).

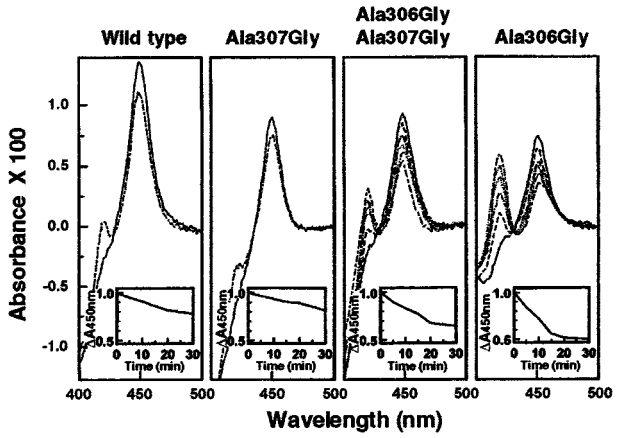

FIGURE 6: Evolution of the CO binding spectra recorded with the sodium dithionite-reduced microsomes from yeasts expressing the wild type and distal mutants of CYP73A1. Microsomes were diluted to 0.4 mg of protein/mL in 0.1 M sodium phosphate buffer (pH 7.4) containing 20% glycerol and reduced with solid sodium dithionite. Difference spectra were recorded 0 (—), 5, 10, 15, 20, and 30 (– - –) min after saturation of the assay cuvette with CO. For the wild type and the Ala307Gly mutant, only the spectra at 0 and 30 min are shown. In the insets are shown graphic representations of the decrease in A_{450nm} vs time. The absorbance recorded immediately after saturation with CO was used as a reference. All spectra were recorded at 30 °C.

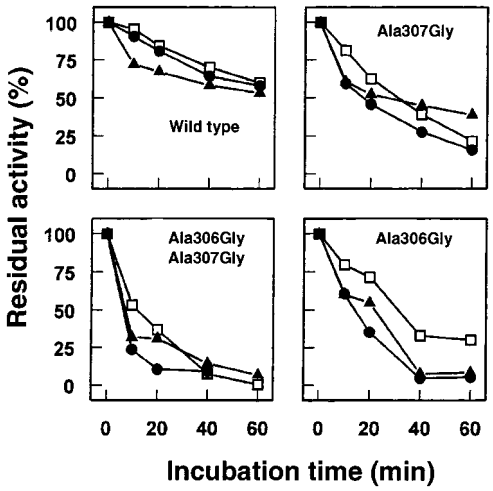

FIGURE 7: Time-dependent inactivation of the wild type and I helix mutants of CYP73A1. Transgenic yeast microsomes were incubated at 30 °C in 0.1 M sodium phosphate buffer alone (▲), in the presence of 500 μM NADPH (●), or in the presence of 500 μM NADPH and 50 μM cinnamate (□), before measuring the residual C4H activity. Data are means of two determinations.

and double mutants, respectively. The decreases in k_{cat} detected for the two Ala306 mutants were correlated to an uncoupling of the reaction.

Stability of the I Helix Mutants. When recording the reduced CO binding spectra, we observed a rapid decrease in the absorbance maximum at 450 nm and a simultaneous increase in the absorption at 420 nm in microsomes of yeast expressing the Ala306Gly mutant. We therefore monitored changes in reduced CO binding spectra as function of time for the wild type and for three modified proteins (Figure 6). A rapid conversion of P450 into the inactive P420 was detected for the Ala306Gly mutant and, to a lesser extent, for the Ala306Gly/Ala307Gly mutant. The extent of conversion in 30 min was around 50% for the T−4 mutant and about 35% for the double mutant. For the wild type and Ala307Gly mutant proteins, decreases in absorbance at 450 nm after incubation for 30 min at 30 °C were similar and very small.

Differences in enzyme stability provided a possible explanation for the differences in enzyme abundance and k_{cat} measured in our experiments. We thus further investigated the stability of the mutants in yeast membranes at 30 °C in their native oxidized forms or in the presence NADPH, alone or in combination with the substrate. The functional integrity of the enzyme was monitored by measurements of catalytic activity. Figure 7 shows that inactivation curves were similar whether the enzyme was incubated alone, in the presence of NADPH, or with NADPH and cinnamate. The extent of inactivation of the wild type enzyme was significant (about 40% in 60 min), but it was relatively slow compared to the inactivation of the modified proteins. The fastest inactivation (about 90% within 40 min) was observed for the two T−4-modified enzymes. The inactivation of the Ala307Gly mutant was intermediate between those of the wild type and of the T−4-modified proteins.

DISCUSSION

Comparison of three-dimensional structures of the crystallized, soluble bacterial P450s reveals that, despite sequence identities of less than 20%, the different proteins clearly possess the same set of secondary structural elements arranged in a very similar overall fold (*13*, *38*). The superposition of Cα backbones and heme groups points to a region of very high structural similarity around the prosthetic group which defines a conserved P450 "core" structure (*13*). This structure is composed of the D, E, and I−L helices, β-sheets 1 and 2, and the heme binding region. The core structure is expected to be found in all P450s. It is probably important for the folding of the protein, the heme binding, and the catalytic functions common to all P450s.

Alignment of sequences from various membrane-bound, eukaryotic P450s (*17*, *39*, *40*) reveals domains that exhibit

higher sequence similarity which are located principally in the C-terminal portion of the proteins. Such regions of high similarity are likely related to conserved structure and catalytic properties common to all P450s. Indeed, when compared to the sequences of the crystallized P450s, these regions map very well on structural elements in the core structure that has been well characterized for the bacterial proteins (*13*, *18*, *41*). In addition, the secondary structure predicted from the primary sequences of various mammalian P450s matches the secondary structure of $P450_{cam}$, even though amino acid sequence identities are only 13% (*42*). Several attempts have been made to build three-dimensional structural models of the membrane-bound P450s with homology building based on the crystal structure of $P450_{cam}$ (*43*−*45*) or on that of other bacterial proteins (*19*, *41*, *46*−*48*). Other authors have used a combination of homology building techniques and site-directed mutagenesis to improve the validity of the models (*49*−*51*). Structural models built for membrane-bound P450s indicate a high variability at the surface of the protein for structures involved in the binding of the redox partner, in docking of the substrate, or in the membrane anchor. The core structure surrounding the heme is, however, very well conserved. The most highly conserved regions are those spanning both sides of the heme surface and those which are directly involved in heme binding or catalysis. Conservation is true, in terms of both structure and sequence (Tables 1 and 2).

The heme is covalently bound to a cysteine which is invariant in all P450 proteins. This cysteine is located in a β-bulge often called the cysteine pocket that seems to envelop the sulfur−iron bond in a hydrophobic environment. The pocket seems to be closed on both sides by highly conserved residues. On the N-terminal side, a phenylalanine residue (C−7) located very close to the sulfur−iron bond completes the hydrophobic enclosure of the proximal side of the heme. On the C-terminal side, a strictly conserved glycine (C+2), allowing for a sharp turn, controls the transition from the cysteine pocket into the L helix and the close approach to the heme. The residue at C+1 is more variable. In most P450s, it is a hydrophobic aliphatic (L, I, V, or A) or aromatic (F) amino acid. In all CYP73As, but also in the majority of plant P450s and in very few bacterial or animal enzymes, for example, CYP104 from *Agrobacterium tumefaciens* or the CYP7 family, this residue is a proline (Table 1). The presence of a proline at this location was unexpected considering the constraints imposed by the conservation of the global core structure and by the key roles of the two adjacent amino acids. To determine if the presence of this proline at C+1 was really important and likely to influence the overall topology of the core, we exchanged proline 448 of CYP73A1 for a valine, an isoleucine, or a phenylalanine.

Modification of the Pro448 led to a drastic loss in enzyme activity (Table 4). This activity loss occurred together (i) with a decrease in CO binding and (ii) with only small uncoupling, since the rate of oxidation of NADPH decreased with C4H activity. Proline mutation thus seems to result in an impaired dioxygen binding and reduction. A dramatic decrease in the substrate-induced shift in heme absorbance was also observed in the microsomes from transgenic yeast expressing the mutant proteins (Figure 3). The most likely explanation of the loss in catalytic function is thus either the absence or a change in the orientation of heme in the active site. To test for the presence of heme, His-tagged mutants were generated, purified, and tested for their specific heme content. Very similar heme-to-protein ratios were measured for the wild type and mutants. Heme is thus present in all mutants, but some folding defect or conformational change alters the interaction between the heme and apoprotein. For all mutants, a small proportion of the protein reaches a functionally active conformation. The active form of the mutants, however, is apparently less stable than the wild type, and in most cases readily converted into P420. Since specific activities of the mutants, expressed on a per P450 only basis, are substantially higher than that of the wild type, the P450 to P420 conversion presumably only occurs after reduction of the enzyme. In the case of the Pro448Phe mutation, and more strikingly in the case of the Pro448Ile mutant, the proline modification also decreased the accumulation of the immunoreactive protein (Figure 2). This may reflect an accelerated degradation of the most unstable conformations of the protein, but may also result from a perturbation in the synthesis of the hemoprotein, involving folding or heme incorporation. The decrease in the steady state level of CYP73A1 transcripts detected in the case of the mutants may reflect difficulties in completely controlling all parameters of the induction process, but may also be indicative of aborted translation due to difficult heme cotranslational incorporation, and resulting in accelerated degradation of the mRNA.

The replacement of Pro448 by a valine was the only modification which led to a more stable protein that was not readily converted into P420. It was also the only mutation for which highest hemoprotein and catalytic activity was detected. This can be taken as an indication that the bulk of the C+1 amino acid side chain may hinder the folding of a correct core structure. However, modeling of the CYP73A1 active site on the basis of the crystallized bacterial proteins, and replacement of Pro448 by Ile, Val, or even Phe, do not show any sign of major steric hindrance that might result from replacement of the pyrrolidine group. The changes in the levels of relative expression observed for the His-tagged mutants also tend to confirm that the size of the C+1 residue side chain is not the most critical determinant of protein stability. Proline is unique among amino acids in that the side chain is cyclized back onto the backbone amide position. This character confers constraints on the peptide chain and restricts the conformational space of the preceding residue. The C+1 proline may thus be critical for reaching a stable conformation. On the other hand, proline is allowed to adopt a cis conformation more easily and more frequently than the 19 other amino acids. In the crystallographically solved structures, the residues at the C+1 position are in a regular trans conformation and there is no indication that Pro448 should behave differently. A cis conformation would require a major rearrangement of the cysteine loop and L helix, but the possibility that Pro448 transiently adopts a cis conformation during the chain folding and heme incorporation cannot be excluded. Proline cis−trans isomerization has indeed been shown to regulate the folding process (*52*, *53*). Finally, a completely conserved CP pair was recently characterized as the heme-binding motif of a wide range of heme-regulated proteins, including the yeast transcriptional activator HAP1, human δ-aminolevulinate synthase, yeast heme lyase, *E. coli* catalase, and rat heme oxygenase-2 (*20*). It was found that

cysteine was absolutely essential for the binding of heme, and that a change of the proline to alanine decreased the affinity of interaction of hemin for a 10-amino acid model peptide mimicking the heme regulatory motif found in these proteins. Such data suggest that proline may also contribute to the incorporation of heme into growing or incompletely folded P450 polypeptide. At the present stage, it is difficult to determine if the decrease in the level of immunodetectable protein observed for the mutants results from an accelerated breakdown of a destabilized hemoprotein or from disrupted translation due either to misfolding or to an inefficient cotranslational incorporation of heme. The slightly lower heme-to-protein ratios observed in the case of the Pro448Val-4His and Pro448Ile-4His mutants, and the easy conversion of some mutants into P420, would support the first hypothesis. The apparent decrease in mutant transcripts would plead for the second. Both mechanisms may actually converge to lead to enzyme loss and inactivation.

The distal side of the heme is spanned by the central part of the I helix. This region corresponds to the second most highly conserved structure in all P450s. It is characterized by a disruption of the normal helical hydrogen bonds that results in the formation of a groove or cleft filled with ordered solvent molecules. This structure is stabilized by a complex set of hydrogen bonds between amino acids or between amino acids and solvent molecules. The amino acids which border the groove seem to play a critical role in the stabilization of the structure and in catalysis. The groove is bordered on the C-terminal side by a highly conserved threonine (T310 in CYP73A1) preceded by a conserved acidic amino acid. The N-terminal border is formed by an alanine (T−4), sometimes by a glycine, which is usually followed by a highly conserved glycine (T−3). In crystallized proteins, the side chain of the conserved threonine forms a hydrogen bond with the carbonyl oxygen atom of the alanine located at T−4, on the other side of the cleft. The carbonyl oxygen of this alanine forms a second hydrogen bond to the axial ligand (water or hydroxide) to the heme iron. When a second threonine is present at T+1 (which is the case for $P450_{BM3}$ and $P450_{terp}$, but also for CYP73A1), a second hydrogen bond is usually observed between the side chain of this threonine and the residue at T−3. The conserved acidic side chain at T−1 forms salt bridges or hydrogen bonds with basic residues close to the surface of the protein. The functions of these conserved residues are probably multiple, and still disputed. When the substrate is bound to the active site, they may provide a binding pocket for diatomic ligands such as dioxygen (*35*). By contributing to the modification of the I helix and to the building of a water channel, or more directly by a mechanism of charge relay, they likely participate in the transfer of protons to the heme-bound reduced dioxygen and to the splitting of the molecule (*13*). In addition, due to their proximity to the reactive center, they have been shown to influence substrate specificity or substrate positioning in the active site (*35*, *54*−*57*).

The role of the hydrophilic amino acids at the C-terminal border of the I helix groove has been extensively investigated by site-directed mutagenesis and crystallographic studies (*54*−*57*, *59*−*65*). Much less is known about the function of the amino-terminal hydrophobic residues. CYP73As all present a divergent amino acid in T−3 (A instead of G) compared to the vast majority (i.e., 95%) of other P450s. This unusual T−3 alanine is also present in a few other plant P450s such as CYP79, CYP71C1, CYP75A1, and CYP90, all of which are involved in the synthesis of molecules with important physiological functions such as defense or signaling, and in a very few bacterial or animal enzymes, including the CYP19 (aromatase) and CYP24 families involved in the synthesis of steroid hormones (Table 2). Our aim in this work was to investigate to role of the highly conserved T−3 glycine, and the reason for its substitution with an alanine in CYP73As, but also to gain an insight into the functions of the T−4 alanine. We thus replaced each or both of the T−3 and T−4 alanines with glycine, creating mutations which seemed to be compatible with the functional core architecture of the enzyme.

Good expression of catalytically active enzyme was obtained for all three mutants (Figure 4 and Table 6). Comparison of the amounts of immunodetected protein and of the relative amplitude of the reduced CO binding spectra did not indicate any major alteration in heme binding (Figure 5). Ala to Gly mutations thus probably had no profound change on the core architecture. Substitution of the T−3 and T−4 residues, however, resulted in changes in substrate binding, catalytic efficiency, and stability of the protein. Measurement of the substrate binding characteristics ($K_{s,app}$ and % of HS) clearly indicated subtle changes in substrate orientation in the active site occurred (Table 5).

The Ala307Gly mutation apparently led to a slightly improved positioning of the substrate in the active site compared to that of the wild type, since the K_s for cinnamate was reproducibly decreased and the sixth ligand to the heme iron was efficiently displaced. An improved catalytic efficiency was thus expected for this mutant. This was actually observed when the kinetic parameters of the hydroxylation reaction were measured (Table 6). The removal of the alanine methyl side chain thus seemed to facilitate substrate access to the catalytic site and positioning close to heme iron. So why was an alanine maintained in T−3 in all CYP73s?

In the absence of crystallographic data, interpretation of these results remains speculative. The removal of the alanine methyl side chain may induce a reorientation in the side chains of adjacent residues, increase the mobility of the substrate, or leave an empty space for an additional molecule of solvent in the active site. It has also previously been suggested that the presence of a glycine or a proline in this or the adjacent position might help to create a bend or a kink in the I helix structure which would establish an optimal fit of the substrate in the catalytic site or help the folding or breathing of the P450 protein (*19*, *50*). Increased mobility does not seem to be a factor considering that the binding constants and catalytic efficiencies are improved, and coupling of NADPH oxidation and substrate hydroxylation is good. The stability of the reduced CO complex (Figure 6), likewise, seems to indicate that there is no perturbation in the interaction of the mutant with diatomic ligands such as dioxygen. CYP73A1, when incubated at 30 °C, is rapidly inactivated in the presence or absence of substrate and of the NADPH cofactor. The inactivation is significantly accelerated in the Ala307Gly mutant. A possible interpretation is that a minor alteration in the geometry of the I helix groove reduces the stability of the core structure. This may occur when an additional molecule of solvent modifies the

hydrogen bond network or when a bend in the helix backbone is introduced. Another possibility is that the hydrophobic alanine methyl side chain helps to prevent uncontrolled solvent proton transfer to the active center and to generate reactive oxygen. Evolution would thus have chosen stability over efficiency.

A very different situation is observed in the case of the Ala306Gly mutant. Substrate binding parameters indicate both a decreased affinity and either an increased mobility or an incorrect positioning of the substrate in the modified active site. The altered substrate binding results in a 6-fold decrease in the catalytic efficiency and in a 5-fold excess in NADPH reduced per hydroxylated cinnamate. The mutation also results in a destabilization of the reduced CO complex that is rapidly converted to P420. Incubated at 30 °C, the enzyme is almost totally inactivated in 40 min. In crystallized structures, the T−4 residue is the I helix amino acid located closest to the heme iron (*13*). It has been shown to directly interact with the substrate (*35*) and to occupy a strategic position at the entrance of the I helix groove, contributing to its structure, to the binding of the axial diatomic ligand, and possibly to the transfer of protons from the distal surface of the protein. The removal of the methyl side chain of Ala306 may thus have multiple consequences. It could result in a looser binding of cinnamate if one of the roles of the side chain is to push the substrate closer to the catalytic iron, thereby establishing a hydrophobic interaction with the cinnamate phenyl ring. This is clearly not the only function of this methyl group. It also seems to be needed to avoid disruption of the heme−protein interaction in the reduced CO diatomic ligand−P450 complex, perhaps by preventing a stretching of the iron−thiolate bond. It could thus also be important for stabilizing the P450−dioxygen complex. Finally, like the Ala307 methyl group, it appears to be necessary in preventing spontaneous enzyme inactivation.

The double alanine to glycine mutation leads to an intermediary situation. Apparently, the removal of the methyl on Ala306 partially compensates for the effect of the removal of the side chain on Ala307. This may be because both methyl groups have opposite steric effects. It is also possible that the removal of both allows the I helix to move a little closer to the heme surface or to slightly close the mouth of the I helix groove, eliminating the formation of empty space and solvent access to the active site. Interestingly, GG motifs, but never any AG motifs in T−3 or T−4, are found in natural P450s. In the case of CYP73A1, the substitution of the two alanines at the N-terminal border of the I helix groove for glycines leads to a rapid inactivation of the enzyme.

Conclusion. In this work, we have demonstrated that the presence of a proline adjacent to the invariant heme binding cysteine is essential for the organization of a correct core structure in CYP73A1. The C+1 residue, therefore, appears to play an important role in ensuring the proper orientation of the heme, and the overall folding and stability of the protein. It may also influence the efficiency of the binding of the heme to the nascent protein. Since many plant P450s and a few animal forms possess the same CPG sequence in the heme-binding region, this motif is probably the landmark of a particular type of core structure.

In contrast, modifying the residues which form the N-terminal edge of the I helix groove, three and four positions upstream of the conserved threonine, generates mutations in this region that (1) influence the binding (affinity and positioning) of the substrate in the active site, (2) deeply affect the stability of the enzyme, whereby removal of either or both of the alanine methyl groups by substitution with glycines leads to rapid and spontaneous inactivation of the enzymes, and (3) in the case of the A to G mutation in T−4 result in the destabilization of the P450−diatomic ligand complex. The presence of a helix-breaking residue N-terminal to the I helix cleft is clearly not essential for building a functional P450 core structure.

Crystallographic data for P450 enzymes exhibiting similar features are needed to provide more accurate structural explanations of these results.

ACKNOWLEDGMENT

We thank Dr. M. Bergdoll for bulding a model of CYP73A1 and for very helpful discussion. We also thank M. F. Castaldi for her technical assistance. The W(R) yeast strain and the pYeDP60 expression vector were kindly provided by Drs. D. Pompon and P. Urban. The critical reading and linguistic improvement of the manuscript by R. Backhaus, R. Kahn, and F. Bernier is gratefully acknowledged.

REFERENCES

1. Nelson, D. R., Koymans, L., Kamataki, T., Stegeman, J. J., Feyereisen, R., Waxman, D. J., Waterman, M. R., Gotoh, O., Coon, M. J., Estabrook, F. J., Gunsalus, I. C., and Nebert, D. S. (1996) *Pharmacogenetics 6*, 1−42.
2. Teutsch, G. H., Hasenfratz, M. P., Lesot, A., Stoltz, C., Garnier, J. M., Jeltsch, J. M., Durst, F., and Werck-Reichhart, D. (1993) *Proc. Natl. Acad. Sci. U.S.A. 90*, 4102−4106.
3. Pierrel, M. A., Batard, Y., Kazmaier, M., Mignotte-Vieux, C., Durst, F., and Werck-Reichhart, D. (1994) *Eur. J. Biochem. 224*, 835−844.
4. Schuler, M. A. (1996) *Crit. Rev. Plant Sci. 15*, 235−284.
5. Werck-Reichhart, D. (1995) *Drug Metab. Drug Interact. 12*, 221−243.
6. Durst, F., and Nelson, D. R. (1995) *Drug Metab. Drug Interact. 12*, 189−206.
7. Poulos, T. L., Finzel, B. C., Gunsalus, I. C., Wagner, G. C., and Kraut, J. (1985) *J. Biol. Chem. 260*, 16122−16130.
8. Ravichandran, K. G., Boddupalli, S. S., Hasermann, C. A., Peterson, J. A., and Deisenhofer, J. (1993) *Science 261*, 731−736.
9. Hasemann, C. A., Ravichandran, K. G., Peterson, J. A., and Deisenhofer, J. (1994) *J. Mol. Biol. 236*, 1169−1185.
10. Cupp-Vickery, J. R., and Poulos, T. L. (1995) *Struct. Biol. 2*, 144−153.
11. Park, S. Y., Shimizu, H., Adachi, S., Nakagawa, A., Tanaka, I., Nakahara, K., Shoun, H., Obayashi, E., Nakamura, H., Iizura, T., and Shiro, Y. (1997) *Nat. Struct. Biol. 4*, 827−832.
12. Poulos, T. L., and Raag, R. (1992) *FASEB J. 6*, 674−679.
13. Hasemann, C. A., Kurumbail, R. G., Boddupalli, S. S., Peterson, J. A., and Deisenhofer, J. (1995) *Structure 3*, 41−62.
14. Nelson, R. D., and Strobel, H. W. (1989) *Biochemistry 28*, 656−660.
15. Von Wachenfeldt, C., and Johnson, E. F. (1995) in *Cytochrome P450: Structure, Mechanism, and Biochemistry* (Ortiz de Montellano, P. R., Ed.) 2nd ed., pp 183−223, Plenum Press, New York.
16. Graham-Lorence, S. E., and Peterson, J. A. (1996) *FASEB J. 10*, 206−214.
17. Kalb, V. F., and Loper, J. C (1988) *Proc. Natl. Acad. Sci. U.S.A. 85*, 7221−7225.

18. Graham-Lorence, S. E., and Peterson, J. A. (1996) *Methods Enzymol. 272*, 315−326.
19. Graham-Lorence, S. E., Amarneh, B., White, R. E., Peterson, J. A., and Simpson, E. R. (1995) *Protein Sci. 4*, 1065−1080.
20. Zhang, L., and Guarente, L. (1995) *EMBO J. 14*, 313−320.
21. Truan, G., Collin, C., Reisdorf, P., Urban, P., and Pompon, D. (1993) *Gene 125*, 49−55.
22. Urban, P., Werck-Reichhart, D., Teutsch, H. G., Durst, F., Mignotte, C., Kazmaier, M., and Pompon, D. (1994) *Eur. J. Biochem. 222*, 843−850.
23. Hoffman, C. S., and Winston, F. (1987) *Gene 57*, 262−272.
24. Devereux, J., Heaberlin, P., and Smithies, O. (1984) *Nucleic Acids Res. 12*, 387−395.
25. Waldon, C., and Lacroute, F. (1975) *J. Bacteriol. 122*, 855−865.
26. Sambrook, J., Fritsch, E. F., and Maniatis, T. (1989) *Molecular cloning: a laboratory manual*, 2nd ed., Cold Spring Harbor Laboratory Press, Plainview, NY.
27. Werck-Reichhart, D., Batard, Y., Kochs, G., Lesot, A., and Durst, F. (1993) *Plant Physiol. 102*, 1291−1298.
28. Omura, T., and Sato, R. (1964) *J. Biol. Chem. 239*, 2370−2378.
29. Omura, T., and Sato, R. (1964) *J. Biol. Chem. 239*, 2379−2385.
30. Schalk, M., Batard, Y., Seyer, A., Nedelkina, S., Durst, F., and Werck-Reichhart, D. (1997) *Biochemistry 36*, 15253−15261.
31. Werck-Reichhart, D., Jones, O. T. G., and Durst, F. (1988) *Biochem. J. 249*, 473−480.
32. Reichhart, D., Salaün, J. P., Benveniste, I., and Durst, F. (1980) *Plant Physiol. 66*, 600−604.
33. Duggleby, R. G. (1984) *Comput. Biol. Med. 14*, 447−455.
34. Raag, R., and Poulos, T. L. (1989) *Biochemistry 28*, 7586−7592.
35. Li, H., and Poulos, T. L. (1997) *Nat. Struct. Biol. 4*, 140−146.
36. Raag, R., and Poulos, T. L. (1989) *Biochemistry 28*, 917−922.
37. Martinis, S. A., Blanke, S. R., Hager, L. P., Sligar, S. G., Hui Bon Hoa, G., Rux, J. J., and Dawson, J. H. (1996) *Biochemistry 35*, 14530−14536.
38. Poulos, T. L., Cupp-Vickery, J., and Li, H. (1995) in *Cytochrome P450: Structure, Mechanism, and Biochemistry* (Ortiz de Montellano, P. R., Ed.) 2nd ed., pp 125−150, Plenum Press, New York.
39. Nelson, R. D., and Strobel, H. W. (1988) *J. Biol. Chem. 263*, 6038−6050.
40. Ouzounis, C. A., and Melvin, W. T. (1991) *Eur. J. Biochem. 198*, 307−315.
41. Chang, Y. T., Stiffelman, O. B., Vasker, I. A., Loew, G. H., Bridges, A., and Waskell, L. (1997) *Protein Eng. 10*, 119−129.
42. Gotoh, O. (1992) *J. Biol. Chem. 267*, 80−90.
43. Laughton, C. A., Neidle, S., Zvelebil, M. J. J. M., and Sternberg M. J. E. (1990) *Biochem. Biophys. Res. Commun. 171*, 1160−1167.
44. Poulos, T. L. (1991) *Methods Enzymol. 206*, 11−30.
45. Koymans, L. M. H., Vermeulen, N. P. E., Baaeslag, A., and Donné-Op den Kelder, G. M. (1993) *J. Comput.-Aided Mol. Des. 7*, 281−289.
46. Ruan, K.-H., Milfeld, K., Kulmacz, R., and Wu, K. K. (1994) *Protein Eng. 7*, 1345−1351.
47. de Groot, M. J., Vermeulen, N. P., Kramer, J. D., van Acker, F. A., and Donné-Op den Kelder, G. M. (1996) *Chem. Res. Toxicol. 9*, 1079−1091.
48. Lewis, D. F., and Lake, B. G. (1996) *Xenobiotica 25*, 585−598.
49. Graham-Lorence, S. E., Khalil, M., Lorence, M. C., Mendelson, C. R., and Simpson, E. R. (1991) *J. Biol. Chem. 266*, 11939−11946.
50. Lin, D., Zhang, L. H., Chiao, E., and Miller, W. L. (1994) *Mol. Endocrinol. 8*, 392−402.
51. Szklarz, G. D., Ornstein, R. L. H., and Halpert, J. R. (1996) *J. Biomol. Struct. Dyn. 12*, 61−77.
52. Vanhoof, G., Goossens, F., De Meester, I., Hendricks, D., and Scharpé, S. (1995) *FASEB J. 9*, 736−744.
53. Bergdoll, M., Remy, M. H., Cagnon, C., Masson, J. M., and Dumas, P. (1997) *Structure 5*, 391−401.
54. Imai, Y., and Nakamura, M. (1989) *Biochem. Biophys. Res. Commun. 158*, 717−722.
55. Furuya, H., Shimizu, T., Hirano, K., Hatano, M., Fujii-Kuriyama, Y., Raag, R., and Poulos, T. (1989) *Biochemistry 28*, 6848−6857.
56. Shimizu, T., Sadeque, A. J. M., Sadeque, G. N., Hatano, M., and Fujii-Kuriyama, Y. (1991) *Biochemistry 30*, 1490−1496.
57. Fukuda, T., Imai, Y., Komori, M., Nakamura, M., Kusunose, E., Satouchi, K., and Kusunose, M. (1993) *J. Biochem. 113*, 7−12.
58. Imai, M., and Nakamura, M. (1988) *FEBS Lett. 234*, 313−315.
59. Imai, M., Shimada, H., Watanabe, Y., Matsushima-Hibiya, Y., Makino, R., Koga, H., Horiuchi, T., and Ishimura, Y. (1989) *Proc. Natl. Acad. Sci. U.S.A. 86*, 7823−7827.
60. Raag, R., Martinis, S. A., Sligar, S. G., and Poulos, T. L. (1991) *Biochemistry 30*, 11420−11429.
61. Chen, S., and Zhou, D. (1992) *J. Biol. Chem. 267*, 22587−22594.
62. Zhou, D., Korzekwa, K. R., Poulos, T., and Chen, S. (1992) *J. Biol. Chem. 267*, 762−768.
63. Ishigooka, M., Shimizu, T., Hiroya, K., and Hatano, M. (1992) *Biochemistry 31*, 1528−1531.
64. Hiroya, K., Murakami, Y., Shimizu, T., Hatano, M., and Ortiz de Montellano, P. R. (1994) *Arch. Biochem. Biophys. 310*, 397−401.
65. Vaz, A. D. N., Pernecky, S. J., Raner, G. M., and Coon, M. J. (1996) *Proc. Natl. Acad. Sci. U.S.A. 93*, 4644−4648.

BI982989W